Radka Keslerová; Karel Kozel

Numerical modelling of viscous and viscoelastic fluids flow through the branching channel

In: Jan Chleboun and Petr Přikryl and Karel Segeth and Jakub Šístek and Tomáš Vejchodský (eds.): Programs and Algorithms of Numerical Mathematics, Proceedings of Seminar. Dolní Maxov, June 8-13, 2014. Institute of Mathematics AS CR, Prague, 2015. pp. 100--105.

Persistent URL: http://dml.cz/dmlcz/702669

*Programs and Algorithms of Numerical Matematics 17*
J. Chleboun, P. Přikryl, K. Segeth, J. Šístek, T. Vejchodský (Eds.)
Institute of Mathematics AS CR, Prague 2015

# NUMERICAL MODELLING OF VISCOUS AND VISCOELASTIC FLUIDS FLOW THROUGH THE BRANCHING CHANNEL

Radka Keslerová, Karel Kozel

CTU in Prague, Faculty of Mechanical Engineering,
Department of Technical Mathematics
Karlovo nám. 13, 121 35 Prague, Czech Republic
Radka.Keslerova@fs.cvut.cz, Karel.Kozel@fs.cvut.cz

**Abstract**

The aim of this paper is to describe the numerical results of numerical modelling of steady flows of laminar incompressible viscous and viscoelastic fluids. The mathematical models are Newtonian and Oldroyd-B models. Both models can be generalized by cross model in shear thinning meaning.

Numerical tests are performed on three dimensional geometry, a branched channel with one entrance and two output parts. Numerical solution of the described models is based on cell-centered finite volume method using explicit Runge–Kutta time integration. Steady state solution is achieved for $t \to \infty$. In this case the artificial compressibility method can be applied.

## 1. Introduction

The flows in the branching channel are encountered in technical sector as well as in biomedical applications. It is to be in human body in the complex branching system of blood vessels. Therefore the numerical modelling of generalized Newtonian and generalized Oldroyd-B fluids flow is very important for medical science. For the viscoelastic character of blood, the blood flows is numerically simulated by Oldroyd-B mathematical model with generalizing by cross model.

Therefore this work is concerned with the numerical solution of generalized Newtonian and generalized Oldroyd-B fluids flow in the branched channel with T-junction with round cross-section.

## 2. Mathematical model

The fundamental system of equations is the system of generalized Navier–Stokes equations for incompressible fluids. This system is based on the system of balance laws of mass and momentum for incompressible fluids

$$\operatorname{div} \boldsymbol{u} = 0 \tag{1}$$

$$\rho\frac{\partial \boldsymbol{u}}{\partial t} + \rho(\boldsymbol{u}.\nabla)\boldsymbol{u} = -\nabla P + \text{div } \mathbf{T} \tag{2}$$

where $P$ is the pressure, $\rho$ is the constant density, $\boldsymbol{u}$ is the velocity vector. The symbol $\mathbf{T}$ represents the stress tensor.

For the different choice of mathematical model the different definition of the stress tensor is used. For viscous flows with the representative of Newtonian fluids the Newtonian model is considered (see e.g. [1], [2])

$$\mathbf{T} = 2\mu\mathbf{D} \tag{3}$$

where $\mu$ is the dynamic viscosity and tensor $\mathbf{D}$ is the symmetric part of the velocity gradient.

In the case of viscoelastic fluids, the simplest viscoelastic model can be used. This model is denoted as *Maxwell model*

$$\mathbf{T} + \lambda_1\frac{\delta \mathbf{T}}{\delta t} = 2\mu\mathbf{D} \tag{4}$$

where $\lambda_1$ is the relaxation time. The symbol $\frac{\delta}{\delta t}$ represents upper convected derivative.

By combination of two mathematical models (Newtonian and Maxwell) the behaviour of mixture of viscous and viscoelastic fluids can be described. This model is called Oldroyd-B model and it has the form

$$\mathbf{T} + \lambda_1\frac{\delta \mathbf{T}}{\delta t} = 2\mu\left(\mathbf{D} + \lambda_2\frac{\delta \mathbf{D}}{\delta t}\right). \tag{5}$$

where symbols $\lambda_1$ is relaxation time and $\lambda_2$ is the retardation time (with dimension of time).

In the system of equations (1) and (2) is on the right hand side the stress tensor $\mathbf{T}$ which can be decomposed to the Newtonian (viscous) part $\mathbf{T}_s$ and viscoelastic part $\mathbf{T}_e$. The tensor $\mathbf{T}_s$ is defined by Newtonian model (3) and the viscoelastic tensor $\mathbf{T}_e$ is defined by Maxwell model (4)

$$\mathbf{T}_s = 2\mu_s\mathbf{D}, \qquad \mathbf{T}_e + \lambda_1\frac{\delta \mathbf{T}_e}{\delta t} = 2\mu_e\mathbf{D}, \tag{6}$$

where

$$\frac{\lambda_2}{\lambda_1} = \frac{\mu_s}{\mu_s + \mu_e}, \qquad \mu = \mu_s + \mu_e. \tag{7}$$

The upper convected derivative $\frac{\delta}{\delta t}$ used in the viscoelastic part of the stress tensor is defined by the relation, for more details see [1]

$$\frac{\delta \mathbf{T}_e}{\delta t} = \frac{\partial \mathbf{T}_e}{\partial t} + (\boldsymbol{u}.\nabla)\mathbf{T}_e - (\mathbf{W}\mathbf{T}_e - \mathbf{T}_e\mathbf{W}) - (\mathbf{D}\mathbf{T}_e + \mathbf{T}_e\mathbf{D}) \tag{8}$$

where $\mathbf{D}$ is symmetric part and $\mathbf{W}$ is antisymmetric part of the velocity gradient

$$\mathbf{D} = \frac{1}{2}(\nabla \boldsymbol{u} + \nabla \boldsymbol{u}^T) = \frac{1}{2}\begin{pmatrix} 2u_x & u_y + v_x & u_z + w_x \\ u_y + v_x & 2v_y & v_z + w_y \\ w_x + u_z & w_y + v_z & 2w_z \end{pmatrix} \tag{9}$$

and

$$\mathbf{W} = \frac{1}{2}(\nabla \boldsymbol{u} - \nabla \boldsymbol{u}^T) = \frac{1}{2}\begin{pmatrix} 0 & u_y - v_x & u_z - w_x \\ v_x - u_y & 0 & v_z - w_y \\ w_x - u_z & w_y - v_z & 0 \end{pmatrix}. \tag{10}$$

These mathematical models for the stress tensor could be generalized. For this case the viscosity is considered as a viscosity function and it's defined by shear-thinning cross model (for more details see [7])

$$\mu(\dot{\gamma}) = \mu_\infty + \frac{\mu_0 - \mu_\infty}{(1 + (\lambda\dot{\gamma})^b)^a}, \quad \dot{\gamma} = 2\sqrt{\frac{1}{2}\text{tr } \mathbf{D}^2} \tag{11}$$

with special parameters $\mu_0 = 1.6 \cdot 10^{-1}$ Pa.s, $\mu_\infty = 3.6 \cdot 10^{-3}$ Pa.s, $a = 1.23$, $b = 0.64$, $\lambda = 8.2$ s.

## 3. Numerical solution

The system of equations (1),(2) is solved by the artificial compressibility method, see [3, 4]). In its simplest form, only the continuity equation is modified by the first term in the following equation

$$\frac{1}{\beta^2}\frac{\partial p}{\partial t} + \text{div } \boldsymbol{u} = 0 \tag{12}$$

where $\beta$ is positive parameter. The inviscid part of modified Navier–Stokes equations is now strongly hyperbolic and can therefore be solved by standard methods for hyperbolic conservation laws. The system including the modified continuity equation and the momentum equations can be written

$$\tilde{R}_\beta W_t + F^c_x + G^c_y + H^c_z = F^v_x + G^v_y + H^v_z + S, \quad \tilde{R}_\beta = \text{diag}(\frac{1}{\beta^2}, 1, \cdots, 1) \tag{13}$$

where $W$ is vector of unknowns, $W = (p, u, v, w, t_{e1}, \ldots, t_{e6})$, $F^c$, $G^c$, $H^c$ and $F^v$, $G^v$, $H^v$ are inviscid and viscous fluxes and $S$ denotes the source term.

Eq. (13) is discretized in space by the finite volume method and the arising system of ODEs is integrated in time by the explicit multistage Runge–Kutta scheme ([5, 6]).

The flow is modeled in a bounded computational domain where a boundary is divided into three mutually disjoint parts: a solid wall, an outlet and an inlet. At the inlet Dirichlet boundary condition for velocity vector is used and for a pressure and the stress tensor Neumann boundary condition is used. At the outlet the pressure value is given and for the velocity vector and the stress tensor Neumann boundary condition is used. The homogeneous Dirichlet boundary condition for the velocity vector is used on the wall. For the pressure and stress tensor Neumann boundary condition is considered.

## 4. Numerical results

This section deals with the comparison of the numerical results of generalized Newtonian and generalized Oldroyd-B fluids flow. Numerical tests are performed in an idealized branched channel with the circle cross-section. Fig. 1 (left) shows the shape of the tested domain. The computational domain is discretized using a structured, wall fitted mesh with hexahedral cells. The domain is divided to 19 blocks with 125 000 cells.

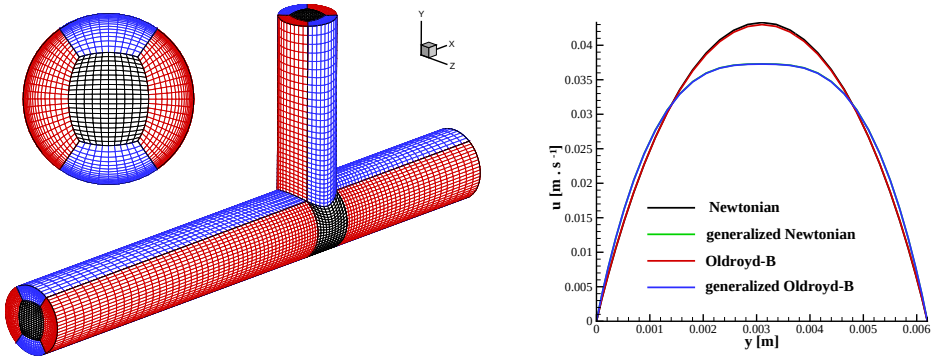


(a) structure of the domain (b) axial velocity profile

Figure 1: Structure of the computed domain (left) and axial velocity profile for steady fully developed flow of tested fluids (right)

As initial condition the following model parameters are used: $\mu_e = 0.0004\,\text{Pa.s}$, $\mu_s = 0.0036\,\text{Pa.s}$, $\lambda_1 = 0.06\,\text{s}$, $U_0 = 0.0615\,\text{m.s}^{-1}$, $L_0 = 0.0031\,\text{m}$, $\rho = 1050\,\text{kg.m}^{-3}$. Using these data, fully developed Poiseuille velocity profile (for Newtonian fluid) is prescribed at the inlet (Dirichlet condition). At the outlet homogeneous Neumann conditions for the velocity components and a constant pressure are prescribed (0.0005 Pa (main channel) and 0.00025 Pa (branch)). On the vessel walls no-slip homogeneous Dirichlet conditions are prescribed for the velocity field. In the case of the Oldroyd-B and generalized Oldroyd-B models, homogeneous Neumann conditions are imposed for the components of the extra stress tensor at all boundaries. In Fig. 1 (right) the axial velocity profile for fully developed flow close to the branching is shown. The lines for Newtonian and Oldroyd-B fluids are similar to the parabolic line, as was assumed. From this velocity profile is clear that the shear thinning fluids attain lower maximum velocity in the central part of the channel (close to the axis of symmetry) which is compensated by the increase of local velocity in the boundary layer close to the wall. In Fig. 2 the velocity isolines and the cuts through the main channel and the small branch for Newtonian fluids are shown.

The axial velocity isolines for all tested fluids are shown in the Figure 3. It can be observed from Fig. 3 that the size of separation region for generalized Newtonian and generalized Oldroyd-B fluids is smaller than for Newtonian and Oldroyd-B fluids.

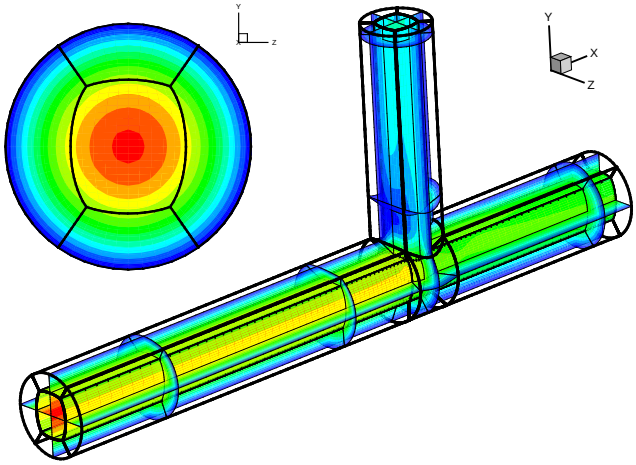


Figure 2: Velocity isolines of steady flows for Newtonian fluids

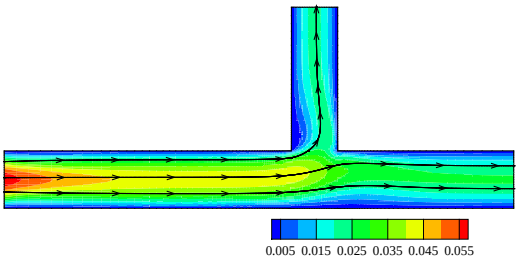


(a) Newtonian

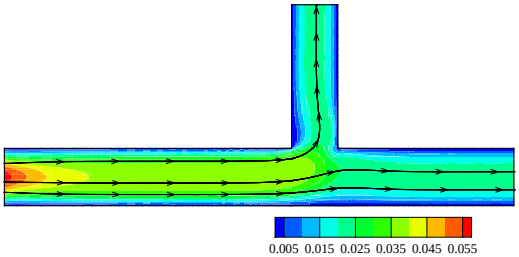


(b) generalized Newtonian

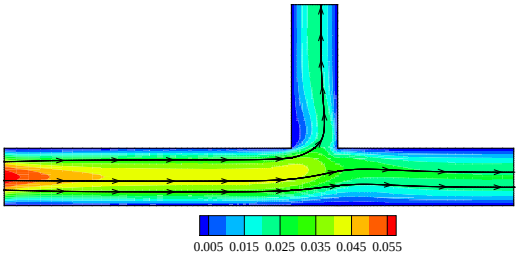


(c) Oldroyd-B

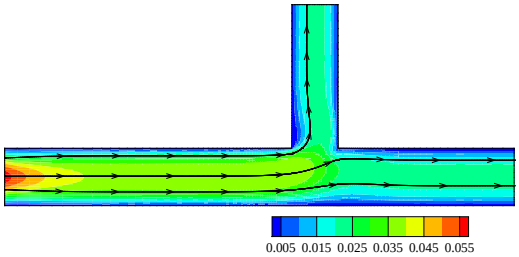


(d) generalized Oldroyd-B

Figure 3: Axial velocity isolines in the center-plane area

## 5. Conclusion

In this paper a finite volume solver for incompressible laminar viscous and viscoelastic flows in the branching channel with T-junction and circle cross section was described. Newtonian and Oldroyd-B fluids models were generalized by the cross model for numerical solution of generalized Newtonian and Oldroyd-B fluids flow. The explicit Runge-Kutta method was considered for time integrating.

The numerical results obtained by this method were presented and compared. In the case of steady flow in this type of the 3D branching channel the numerical results for Newtonian and Oldroyd-B fluids are similar. Future work will be devoted to an extension of this numerical study to the unsteady simulation.

**Acknowledgements**

This work was supported by grant SGS13/174/OHK2/3T/12 of the Czech Science Foundation.

**References**

[1] Bodnar, T., Sequeira, A., and Prosi M.: On the shear-thinning and viscoelastic effects of blood flow under various flow rates. Appl. Math. Comput. **217** (2010), 5055–5067.

[2] Bodnar, T. and Sequeira, A.: Numerical study of the significance of the non-Newtonian nature of blood in steady flow through stenosed vessel. Adv. Math. Fluid Mech. (2010), 83–104.

[3] Chorin, A. J.: A numerical method for solving incompressible viscous flow problem. J. Comput. Phys. **135** (1967), 118–125.

[4] Dvořák, R. and Kozel, K.: *Mathematical modelling in aerodynamics*. CTU in Prague, Czech Republic, 1996.

[5] Keslerová, R. and Kozel, K.: Numerical modelling of incompressible flows for Newtonian and non-Newtonian fluids. Math. Comput. Simulation **80** (2010), 1783–1794.

[6] LeVeque, R.: *Finite-volume methods for hyperbolic problems*. Cambridge University Press, 2004.

[7] Vimmr, J. and Jonášová, A.: Non-Newtonian effects of blood flow in complete coronary and femoral bypasses. Math. Comput. Simulation **80** (2010), 1324–1336.